



*Dedicated to Professor Ionel Haiduc
on the occasion of his 75th anniversary*

EXCIMER LASER-INDUCED SURFACE MODIFICATION OF POLY(ETHYLENE TEREPHTHALATE)

Cristian URSU,^{a,*} Irina BORDIANU,^a Marius DOBROMIR,^b Mioara DROBOTA,^a
Corneliu COTOFANA,^a Mihaela OLARU^a and Bogdan C. SIMIONESCU^{a,c}

^a"Petru Poni" Institute of Macromolecular Chemistry, 41 A Gr. Ghica Voda Alley, 700487 Iași, Roumania

^b"Al. I. Cuza" University, Faculty of Physics, 11 Carol I Blvd., 700506 Iași, Roumania

^cDepartment of Natural and Synthetic Polymers, "Gh. Asachi" Technical University of Iași, 73 D. Mangeron Blvd.,
700050 Iași, Roumania

Received August 11, 2011

The effects on chemical and physical properties of biaxial stretched poly(ethylene terephthalate) (PET) as a result of KrF (248 nm) and XeCl (308 nm) laser irradiation were investigated. Below ablation threshold, roughening of the surface was detected, with the formation of periodic surface structures for 308 nm irradiation, while above the ablation threshold, dendrites or granular protuberances superimpose the densely-packed nap structures. The changes in surface properties were investigated by scanning electron microscopy (SEM) and X-ray photoelectron spectroscopy (XPS). The obtained results suggest that the texture types originate from different contribution rates of photothermal and photochemical mechanisms.

1. INTRODUCTION

Research on intense UV laser interaction with polymers begins with the first two papers published by Srinivasan and co-workers in 1982¹ that put the bases of the applications currently meet today in microelectronics, optics and medicine.² Under UV laser radiation, the polymer surface can be modified in a controlled manner to induce specific functionalities. Surface texture effects of laser irradiation are certainly a concern in many applications for adhesion improvement of coatings,³ particularly in biological applications where mechanical adhesion could represent the first step in attaching cells to biomaterial surfaces.⁴

Generally, semicrystalline polymers have a preferential tendency to form regular microstructures when exposed to UV laser radiation.⁵ Different mechanisms for the formation

of periodic surface structures in excimer laser irradiation experiments have been proposed in the literature. The presence of particulate impurities in polymer films, as well as preferential etching of amorphous and crystalline regions in stretched polymer samples are considered to be the origin of surface texturing,⁶ while Dunn and Ouderkirk⁷ proposed that texture formation is most likely due to the anisotropic strain created in the laser amorphization process which begins with the first exposure pulses.

The present paper deals with a comparative study on surface properties of PET samples after irradiation with two excimer lasers. The obtained results demonstrate that different acting mechanisms are at the origin of structure formation. Moreover, a new type of surface structure (independent fractal objects with a branched appearance – dendrites developed in vertical direction) superimposed onto

* Corresponding author: cristian.ursu@icmpp.ro

close-packed naps obtained after excimer-laser irradiation in ambient atmosphere, is reported (these types of structures normally develop just after irradiation in vacuum).

2. RESULTS AND DISCUSSION

Modifications of PET surface after laser irradiation were investigated in order to determine their nature as well as their evolution with process parameters. SEM images were taken after irradiation with KrF and XeCl lasers with fluencies below (Fig. 1) and above the ablation threshold (Fig. 2) after various pulse numbers. After exposure to an energy density below the ablation threshold, *i.e.*, 26 mJ/cm² for KrF laser (Fig. 1a) and 148 mJ/cm² for XeCl laser (Fig. 1b), roughening of PET surface was detected, as well as the formation of periodic surface structures in the latter case. After increasing the fluence from 148 to 155 mJ/cm², which is still below the ablation threshold, fractal objects with a branched appearance (dendrite type structure) can be evidenced, where each structure seems to grow from a central point through branching (Fig. 1c). Crystallization of the laser-induced amorphous layer was considered to be the driving force of the dendrite growth,¹⁰ but recent results indicate that debris are also important, at least for the nucleation of the structures.¹¹

As a consequence of the KrF laser irradiation for an energy density slightly above the ablation threshold (50 mJ/cm², Fig. 2a), a progressive change in the morphology from a textured surface characterized by the presence of isolated “nap” (5 pulses) to densely-packed structures (150 pulses) with growing nap sizes has been registered. With increasing the pulse number, the naps reach a higher size and on the top of these ones additional materials in the form of a dendritic “appearance” (*i.e.*, a tree-like one) developed in vertical direction can be observed. The dendrites on the top of the

naps are the result of further polymer decomposition – decomposition of the crosslinked polymer or complete decomposition of the ablated fragments which are redeposited.

After laser ablation with 100 pulses, self-assembled, close-packed naps (resembling cones in shape) occur in the PET film. As for the XeCl laser irradiation, the resulted surface morphology is quite different, and a periodically granular structure appears (Fig. 2b). Initial laser shots lead to ripple formation (Fig. 1b). Increasing the irradiation dose, the fragmentation of the periodical chains leads to a long-period naps structure, with some granular protuberances developed onto the top. As opposite to the observed naps for KrF laser irradiation, these ones are larger (from units to tens of micrometers, respectively).

The XPS technique was used to study the surface composition of laser irradiated PET samples. The O/C ratio was derived from the survey spectra. Generally, the O/C ratio decreases for both laser irradiation wavelengths below (Table 1) and above (Table 2) the ablation threshold with a peculiar behavior at 148 mJ/cm², where an initial decrease of the oxygen content is followed by an increase after 100 laser pulses. More detailed results were obtained from the high resolution spectra. The C1s spectrum was fitted with four distinctly resolved peaks corresponding to carbon atoms involved in the C-C, C-H phenyl ring (C₁) and contamination species, carbon of H₂C-O-ether/alcoholic group (C₂), carbon involved in O=C-O-ester/carboxyl group (C₃) and C₄ component (negligible intensity) due to a π - π^* shake-up satellite in phenyl groups, respectively. The O1s spectrum was fitted with two contributions: carbonyl oxygen (O₁, C=O) and singly bonded oxygen (O₂, C-O-).¹²

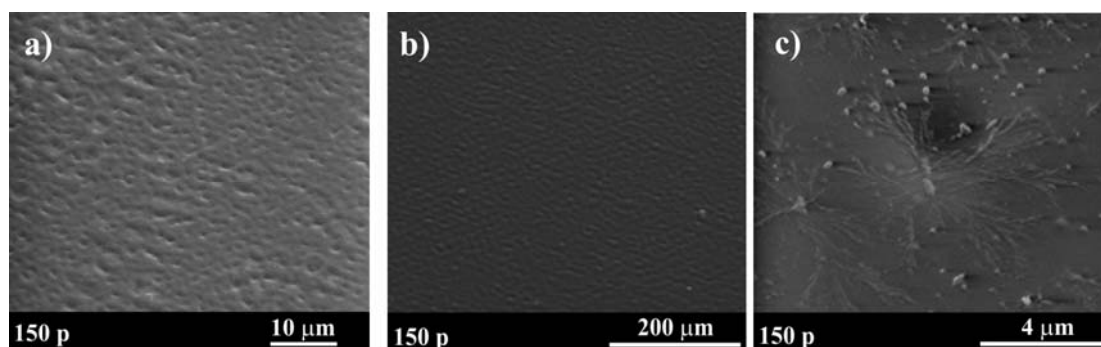


Fig. 1 – Scanning electron microscopy images of PET laser treated samples below the fluence threshold at a) 26 mJ/cm² (KrF), b) 148 mJ/cm² and c) 155 mJ/cm² (XeCl) for 150 pulse number.

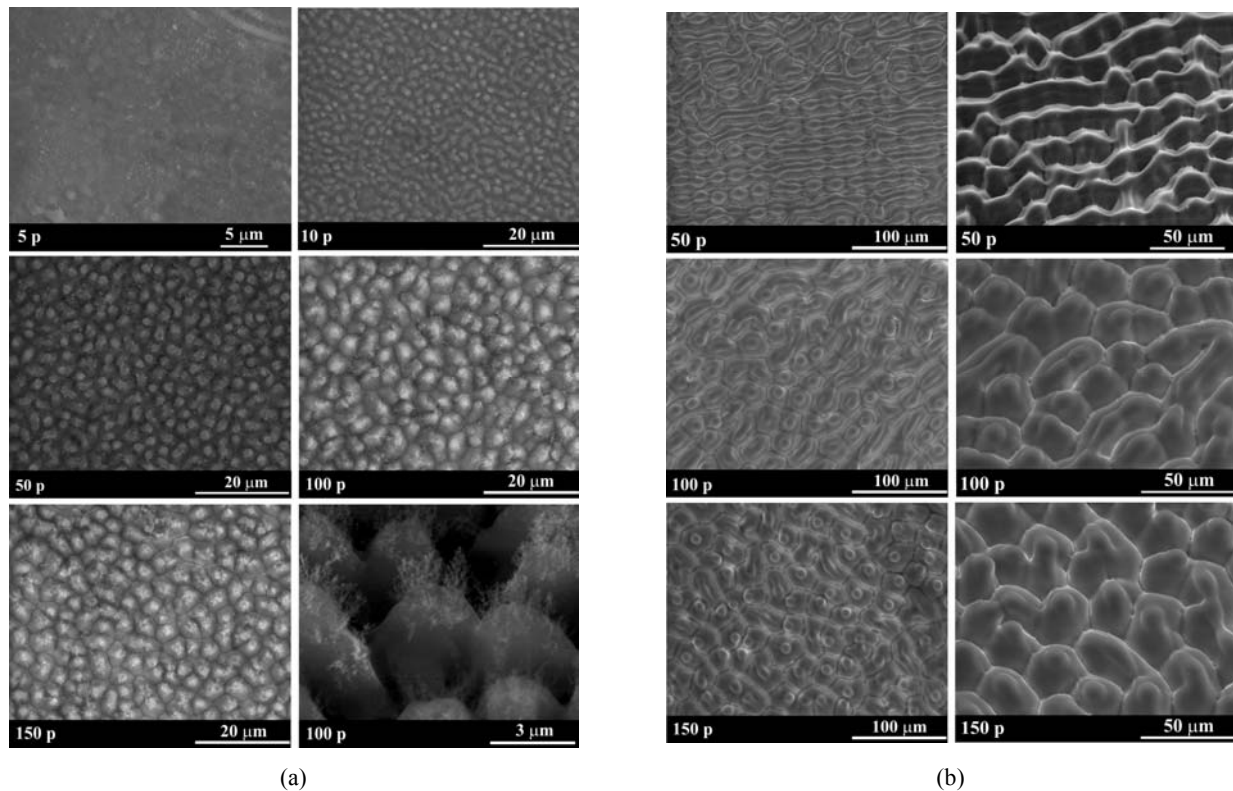


Fig. 2 – Scanning electron microscopy images of PET laser treated samples at a) 50 mJ/cm² (KrF) and b) 283 mJ/cm² (XeCl).

Table 1

Surface composition (C, O atomic percent and C₁/C, C₂/C, C₃/C, C₄/C, O₁/O, O₂/O, O/C ratios) for untreated, T₅, T₁₀₀ and T₁₅₀ treated PET samples (F<F_T)

Sample Fluence (mJ/cm ²)	Untreated PET	T ₅		T ₁₀₀		T ₁₅₀	
		26	148	26	148	26	148
C1s (%)	71.3	75.2	72.6	80.4	67.2	83.2	76.2
O1s (%)	28.7	24.8	27.4	19.6	32.8	16.8	23.8
O/C	0.40	0.33	0.38	0.24	0.49	0.2	0.31
C ₁ /C	64.06	71.64	84.96	76.90	50.83	78.09	71.18
C ₂ /C	18.27	13.68	13.08	12.82	39.45	12.88	13.63
C ₃ /C	16.26	12.75	1.96	7.24	9.51	7.37	13.09
C ₄ /C	1.41	1.92	0.00	3.04	0.21	1.67	2.10
O ₁ /O	47.81	49.68	79.14	44.57	79.08	47.19	46.87
O ₂ /O	52.19	50.32	20.86	55.43	20.92	52.81	53.13

Table 2

Surface composition (C, O atomic percent and C₁/C, C₂/C, C₃/C, C₄/C, O₁/O, O₂/O, O/C ratios) for untreated, T₁, T₅, T₁₀₀ and T₁₅₀ treated PET samples (F>F_T)

Sample Fluence (mJ/cm ²)	Untreated PET	T ₁		T ₅		T ₁₀₀		T ₁₅₀	
		50	283	50	283	50	283	50	283
C1s (%)	71.3	78.4	72.7	80.9	74.8	83.9	74.9	85.7	76.2
O1s (%)	28.7	21.6	27.3	19.1	25.2	16.1	25.1	14.3	23.8
O/C	0.40	0.28	0.38	0.24	0.34	0.19	0.34	0.17	0.31
C ₁ /C	64.06	76.64	65.57	73.07	68.81	78.21	70.89	71.87	69.16
C ₂ /C	18.27	10.35	17.01	18.83	14.83	13.90	13.60	17.04	14.67
C ₃ /C	16.26	10.44	15.29	6.75	14.62	6.61	13.50	7.96	14.49
C ₄ /C	1.41	2.57	2.13	1.35	1.74	1.28	2.01	3.14	1.67
O ₁ /O	47.81	49.63	45.94	61.75	44.95	57.81	45.93	39.57	40.35
O ₂ /O	52.19	50.37	54.06	38.25	55.05	49.19	54.07	60.43	59.65

After PET irradiation with KrF at 26 mJ/cm² (below the ablation threshold), the same behavior was registered between 5-150 pulses, *i.e.*, a decrease of O/C, C₂/C, and C₃/C ratios, and an increase of C₁/C one. After 5 pulses, an increase of O₁/O ratio and a decrease of the O₂/O one were registered as compared to the corresponding values for the initial PET samples (formation of ketone groups and a slight reduction of ether/alcohol subgroups), while after 150 pulses, a decrease of O₁/O ratio and an increase of the O₂/O one were registered (scission of O=C-O groups leading to CO and CO₂ elimination, process correlated with a decrease of the oxygen content on the surface¹³). These results indicate a weak surface decarboxylation, *i.e.*, partially removal of the ester/carboxyl and ether/alcohol functional groups in favor of ketone groups and a marked increase of the amount of C-C, CH aliphatic groups.

Between 5-100 pulses (XeCl, 148 mJ/cm²), laser irradiation leads to a marked increase of O/C and C₂/C (ether species) ratios, while the fractions of benzenic/aliphatic groups (C₁/C) and C₃/C decrease significantly. This result could be correlated with a partial oxidation of PET benzene rings, *i.e.*, presence of benzenic/aliphatic fragments at the PET interface, formed by scission reactions during the laser treatment that can partly undergo re-oxidation, with the formation of new polar ether/alcohol functional groups and decrease of the number of ester/carboxyl units. On the other hand, the increase of O₁/O ratio and the decrease of the O₂/O one indicate the formation of ketone units and a slight reduction of ether/alcohol subgroups. As follows, one can conclude that XeCl laser treatment, below ablation threshold induces a loss of C=O groups and reduces their orientation relative to the surface, as a consequence of thermally-induced amorphization.

In the up-threshold fluence regime for both laser wavelengths, all measurements evidenced the same behavior, *i.e.*, the decrease of the O/C ratio and the increase of C₁/C one. This behavior is correlated with the surface decarboxylation (carbonization of PET surface), *i.e.*, a partial removal of the ester/carboxyl and ether/alcohol functional groups with the formation of ketone units (irradiation up to 100 pulses) or CO and CO₂ due to scission of O=C-O groups (irradiation from 100 to 150 pulses), leading to a marked increase of the amount of C-C and CH aliphatic groups. As follows, the removal of PET fragments produces densely-packed nap structures with different

morphologies (appearance of dendrites or granular protuberances onto the top of naps). These structures are the result of further polymer decomposition and surface carbonization.

The most important chemical changes seem to be related to the first irradiation sequences for both lasers (with a more pronounced influence on KrF treated PET and a less pronounced amorphization than the ones exposed to XeCl irradiation). The amorphization may result from the implication of both chemical changes and thermal effects. Thus, one can speculate that the different texture types originate from different contribution rates of the photothermal and photochemical mechanisms.

3. EXPERIMENTAL

Two excimer lasers (Compex Pro 205 F – KrF and LPX Pro 220 – XeCl working at 248 nm and 308 nm, respectively) were independently used to irradiate biaxially stretched semicrystalline PET foils from Goodfellow (42 % crystallinity and 30 μm thickness, data provided by the producer). PET samples were submitted to laser radiation at normal incidence in atmospheric conditions and at 1 Hz pulse repetition frequency. Prior to laser exposure, the samples were ultrasonically cleaned for 5 minutes, in a bath containing 10 % acetone and water, and then dried in air. Two laser fluence ranges, below (26 mJ/cm² for KrF and 148 mJ/cm², 155 mJ/cm² for XeCl laser) and above (50 mJ/cm² and 283 mJ/cm² for KrF and XeCl laser, respectively) the fluence thresholds, F_T ^{8,9} and different pulses numbers (1, 5, 10, 50, 100 and 150) were used. To ensure a uniform irradiation spot, a 3 x 3 mm² of KrF laser beam was selected by using a mask, while for XeCl laser, the 3 x 3 mm² uniform spot on the surface was assured by the VarioLas system.

SEM investigations of the laser treated PET samples were performed with a QUANTA 200 instrument. XPS measurements were performed on a PHI 5000 VersaProbe Φ ULVAC-PHI Inc spectrometer. An AlKα excitation source (photon energy 1486.7 eV, 100 μm beam size diameter) was used for excitation. Survey spectra (250–850 eV) and high-resolution spectra were recorded for the pass energy of 117.4 and 58.7 eV, respectively, in operation conditions typical for this technique (pressure in the sample chamber ≈ 10⁻⁷ Torr).

4. CONCLUSION

As demonstrated through different surface analysis techniques, PET surface was selectively modified with different laser irradiation wavelengths. For laser irradiation below ablation threshold, roughening of the PET surface was evidenced, with the formation of periodic surface structures for XeCl irradiation. For the fluencies above the ablation threshold, pronounced differences were revealed between the created naps microstructures. The formation of dendrites (KrF)

or granular protuberances (XeCl) on the top of the close-packed naps is the result of further polymer decomposition and surface carbonization. The most important chemical changes and amorphization of the irradiated surface took place for the first irradiation sequences. The different textures may originate from different contribution rates of photothermal and photochemical mechanisms.

Acknowledgements: This work was financially supported by the European Social Fund – “Cristofor I. Simionescu” Postdoctoral Fellowship Programme (ID POSDRU/89/1.5/S/55216), Sectoral Operational Programme Human Resources Development 2007-2013.

REFERENCES

1. R. Srinivasan and V. Mayne-Banton, *Appl. Phys. Lett.*, **1982**, *41*, 576-578.
2. R. Srinivasan and W. J. Leigh, *J. Am. Chem. Soc.*, **1982**, *104*, 6784-6785.
3. A. T. Barfknecht, J. P. Partridge, C. J. Chen and C. Y. Li, “Advanced Electronic Packaging Materials”, Mater. Res. Soc. Proc. 167. Materials Research Society, Pittsburgh, 1990.
4. I. Higashikawa, M. Nonaka, T. Sato, M. Nakase, S. Ito, K. Horioka and Y. Horiike, in D. J. Ehrlich, G. S. Higashi and M. M. Oprysko (Eds.), “Laser and Particle-Beam Chemical Processing for Microelectronics”, Mater. Res. Soc. Proc. 101, Materials Research Society, Pittsburgh, 1990, p. 3-12.
5. D. Bäuerle, E. Arenholz, J. Heitz, S. Proyer, E. Stangel and B. Lukyanchuk, in M. Briege, H. Dittrich, M. Klose, H.W. Schock and J. Werner (Eds.), “Semiconductor Processing and Characterization with Lasers”, Materials Science Forum, Trans Tech Publications, Switzerland, 1995, p. 173-174.
6. T. Lippert, T. Nakamura, H. Niino and A. Yabe, *Macromolecules*, **1996**, *29*, 6301-6309.
7. T. Lippert, F. Zimmermann and A. Wokaun, *Appl. Spec.*, **1993**, *47*, 1931-1942.
8. Y. Novis, J. J. Pireaux, A. Brezini, E. Petit, R. Caudano, P. Lutgen, G. Feyder and S. Lazare, *J. Appl. Phys.*, **1988**, *64*, 365-370.
9. D. S. Dunn and A. J. Ouderkerk, *Macromolecules*, **1990**, *23*, 770-774.
10. H. Niino and A. Yabe, *J. Photochem. Photobiol. A: Chem.*, **1992**, *65*, 303-312.
11. E. Arenholz, M. Wagner, J. Hertz and D. Bäuerle, *Appl. Phys. A.*, **1992**, *55*, 119-120.
12. G. Beamson and D. Briggs, “High resolution XPS of organic polymers”, The Scienta ESCA300 Database, vol. 174, Wiley, 1992, p. 172.
13. S. Petit, P. Laurens, M. G. Bathes-Labrousse, J. Amouroux and F. Arefi-Khonsari, *J. Adhes. Sci. Technol.*, **2003**, *17*, 353-268.